Sci.Int.(Lahore),28(2),1975-1986 ,2016 ISSN 1013-5316;CODEN: SINTE 8

STRETCHING, FIXED AND POROUS MEDIA FINS IN DOUBLE PIPE AND PARALLEL PLATES WITH OPTIMUM DESIGN FOR THERMAL PERFORMANCE

Farooq Ahmad
Department of Mathematics, College of Science, Al-Zulfi, Majmaah University, Saudi Arabia
(Department of Mathematics, Govt. Islamia College, Civil Lines, Lahore, Punjab, Pakistan)
f.ishaq@mu.edu.sa; farooqgujar@gmail.com

ABSTRACT: *Shape design of a fin for optimum thermal performance is investigated by using a computational procedure based on body fitted grid generation, steady conjugate gradient method and grid redistribution scheme. Steady laminar and fully developed flow of incompressible fluid is considered in the annulus of two concentric circular tubes subject to* $\frac{H_1}{T_1}$ *boundary conditions applied at the inner surface. Straight and longitudinal fins are augmented to the outer surface of the inner tube with initial shape being such that the sides lie along the radial lines and the tip forms a circular arc concentric with the tubes. The shape of the fin is iteratively adjusted so that the heat transfer coefficient* Nu *Nusselt number reaches a specified level of performance relative to that for the initial shape. The tests are performed with for a range of values of the parameters the number of fins and the fin height to achieve various levels of thermal performance. The results indicate up to* 20% *increase in the heat transfer coefficient* Nu *Nusselt number for the optimal shape as compared to the initial shape for various configurations of the finned annulus.*

KEYWORDS: Optimal Shape, Curvilinear Grid, Conjugate Gradient, Redistribution Method.

1. INTRODUCTION

The study of optimal shape design can be arrived as by asking the following question, what is best shape for a physical system? This study is of physical systems; in particular, which can be described by an elliptic partial differential equation and where shape is found by the steepest descent, conjugate method and direct sensitivity method.

Traditionally, optimal shape design has been treated as a branch of variations and more specifically of optimal control. This subject interfaces with no less than five fields: body fitted grid generation, optimization, optimal control, partial differential equations, and their numeric solutions; this is the most difficult aspect of the subject. In fact optimization is the act of obtaining the best result under given circumstances. Depending upon the physical structure of the problem, optimization problem can be classified as optimal control and non-optimal control problems

An optimal control system is usually described by two types of the variables, namely, the control (design) and the state variables. The control variables govern the evolution of the system from one stage to the next and the state variables describe the behavior of the system in any stage. Explicitly the optimal control problems in mathematical programming problem involving a number of the stages, where each stage evolves from the previous stage in a prescribed manner.

In mathematical point of view, we define the optimal shape design in the following way:

Let ϕ be the solution of a partial differential equation in a domain Ω;

$$\phi(x) \in R^n \quad \forall \in \Omega \subset R^n. \qquad (1)$$

Let E (ϕ, Ω) be a real-valued function of ϕ on Ω. We may say that we have an optimal shape design problem to solve if we find Ω, in a class Θ of allowable domain, to minimize E. Symbolically, we may write:

$$\min_{\Omega \in \Theta} \{E(\phi, \Omega) : A(\phi, \Omega) = 0\}, \qquad (2)$$

Comparison chart between the Conventional and Optimum Design Process is given below:

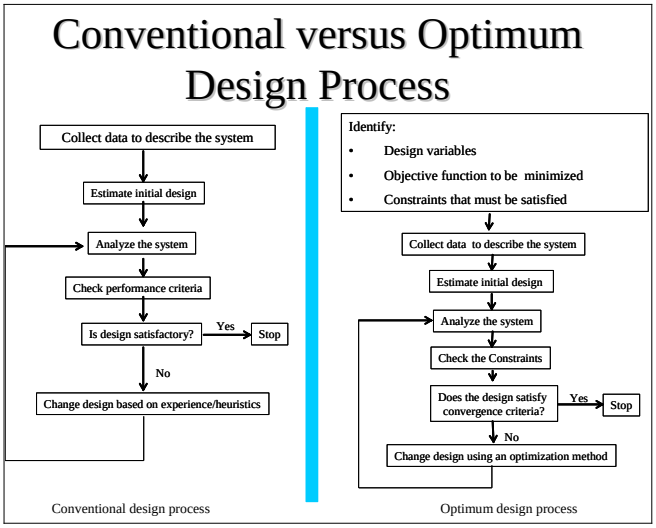

where A is an operator that, for every $\Omega \in \Theta$, defines a unique ϕ. In reality, this definition is too restrictive; broadly speaking, we use the term optimal shape design when-ever a function is to be minimized with respect to a particular geometric element appearing in a partial differential equation.

In 2000, Cheng and Wu [4] proposed an optimization process by combining the body-Fitted grid generation and the CG methods for shape design. In their study, attention was focused on the development of a direct differentiation

scheme for the sensitivity analysis. However, it is noted that since in [4] only the simply connected domains are dealt with, the validity of the numerical schemes for the multiply-connected domains remains unclear. Furthermore, as observed by Cheng and Wu [4], an oscillation of the iterative solution occurs during the iteration process for some particular cases. To avoid the oscillation, a multistage operation was suggested by the authors. In the multistage operation, the solution process from the initial shape to the optimal one is divided into a couple of stages by properly setting a number of intermediate conditions. When an intermediate solution for a stage has been solved, the obtained solution is treated as the initial guess for the next stage. The process proceeds from one stage to another until the desired solution is reached.

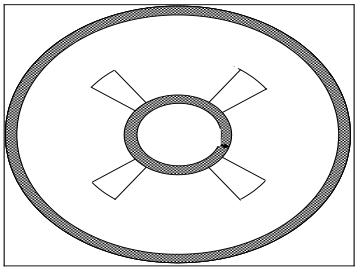

Cross-Section of Finned Double Pipe

Fig. 1

In 2001, C. H. Lan et al. [5] provided a number of test problems with multiply-connected domains are considered to demonstrate the performance of the method presented by Cheng and Wu [4]. Meanwhile, they proposed distribution method to regularize the ill-ordered grids, which are commonly found in the optimization process, to improve the grid quality for the subsequent iterations and hence avoid the oscillation of the solution. Minimization of the objective function is achieved by using the CG method. The curvilinear grid generation scheme requires less implementation efforts and, therefore, it is integrated into the shape-optimization procedure.

Recently in 2007, K. S. Syed et al. [6] solved a problem for convective heat transfer in the thermal entrance region of finned double-pipe.

The study of one-dimensional annular flow is extended to the two-dimensional problem of the steady laminar fully-developed flow of a viscous incompressible fluid moving in the annular region between two concentric pipes with tapered fins augmented to the outer surface of the inner pipe: a finned double pipe (FDP). The fins are assumed to be smooth, straight and equally spaced. Their sides form radii of the circular geometry and the tips are circular arcs concentric with the pipes. A cross-section of the annular domain is shown in Fig.1. The governing momentum equation is solved numerically and the velocity distribution and other flow characteristics are studied for a range of the values of the geometrical parameters: the ratio of the radii, the number of fins, the fin height and the fin thickness.

2. PROBLEM STATEMENT

The system comprises two concentric pipes with longitudinal fins, of zero thickness [24], distributed uniformly around outer surface of the inner pipe while cold fluids flow in the finned annular region. The fluid is viscous, incompressible, Newtonian, and has constant properties. The flow is assumed to be steady, laminar, hydro dynamically fully developed and thermally developing. Here viscous dissipation is negligible. All the body forces are negligible. The only driving force is the pressure gradient in the axial direction. Under the thin fin assumption, the cross-sectional area occupied by the fins is quite negligible as compared to the free flow area. This is a valid assumption and has been taken in many studies like [6, 24, 25,26]. Therefore we assume that the fin thickness is zero. The axial conduction in wall and fluid is neglected. The fin material has infinite conductivity i.e. the fin is 100% efficient. An adiabatic thermal condition is imposed at the outer pipe.

The geometry for parallel plates is to be considered as special case of the two concentric circular tubes/pipes with considers devotion of curvature.

Under the assumptions described above the momentum and energy equations are solved numerically for a range of values of the geometrical parameters; namely the ratio of radii of the inner and the outer pipes, the fin height and the number of fins. The heat transfer results are sought for the uniform heat input per unit axial length with circumferential uniform wall (tube and fins) temperature classified as H_1 boundary condition by [27]. A cross-section of the geometry under consideration is as shown in the fig. 2 & fig. 3 . The geometrical symmetry requires the problem to be solved in the region shown in fig. 4 .

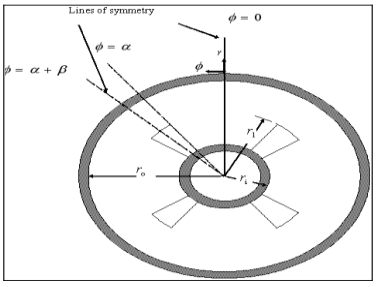

Cross-Section of Finned Double Pipe

Fig. 2

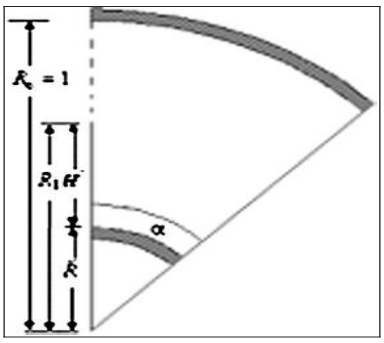

Fig. 3

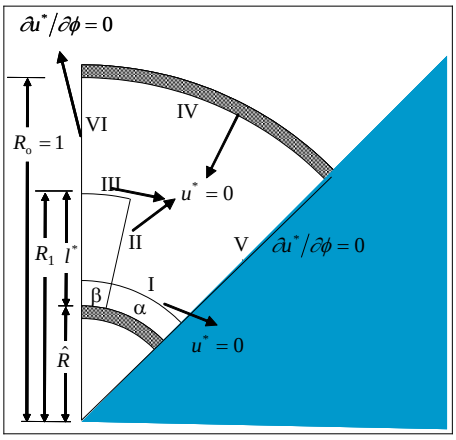

Fig. 4

3. MODELING THE FLUID MOTION

a. Momentum Equation

Under the earlier assumptions, the governing momentum equation for the $2-D$ flow can be written as [6],

$$\frac{\partial^2 u}{\partial^2 r}+\frac{1}{r}\frac{\partial u}{\partial r}+\frac{1}{r^2}\frac{\partial^2 u}{\partial^2 \phi}=\frac{1}{\mu}\frac{dp}{dz}, \qquad (3)$$

where u is the axial velocity component, p is the pressure and z is the axial distance.

The geometrical symmetry requires this to be solved only in the region where $r_i \le r \le r_0$ and $0 \le \phi \le \alpha+\beta$. The dimensionless numerical domain is shown in Fig. 4.

Using the following dimensionless variables:

$$u^* = \frac{u}{u_{\max}},\quad R = \frac{r}{r_0},\quad \hat{R} = \frac{r_i}{r_0},\quad R_1 = \frac{r_1}{r_0}, \qquad (4)$$

and

$$u_{\max} = -\frac{1}{4}\frac{dp}{dz}r_0^2\left(1-R_m^2+2R_m^2\ln R_m\right), \qquad (5)$$

the equation (3) can be reduced to the dimensionless form

$$\frac{\partial^2 u^*}{\partial R^2}+\frac{1}{R}\frac{\partial u^*}{\partial r}+\frac{1}{R^2}\frac{\partial^2 u^*}{\partial \phi^2}=\frac{4}{C}, \qquad (6)$$

where

$$C = -\left(1-R_m^2+2R_m^2\ln R_m\right), \qquad (7)$$

And

$$R_m = \frac{r_m}{r_0} = \sqrt{\frac{1-\hat{R}^2}{2\ln\left(\frac{1}{\hat{R}}\right)}}. \qquad (8)$$

The boundary conditions introduced by the symmetry of the domain and the viscous nature of the fluid can be expressed in dimensionless form as follows:

(a) No-slip conditions at the solid boundaries I-IV

I) $u^* = 0$ at $R = \hat{R},\quad 0 \le \phi \le \alpha,$

II) $u^* = 0$ at $\phi = \alpha,\quad \hat{R} \le R \le R_1,$

III) $u^* = 0$ at $R = R_1, \alpha \le \phi \le \alpha+\beta,$

IV) $u^* = 0$ at $R = 1,\ 0 \le \phi \le \alpha+\beta.$

(b) Symmetry conditions at the lines of symmetry V and VI

V) $\frac{\partial u^*}{\partial \phi} = 0$ at $\phi = 0,\ \hat{R} \le R \le 1,$

VI) $\frac{\partial u^*}{\partial \phi} = 0$ at $\phi = \alpha+\beta,\ R_1 \le R \le 1,$

where R_1 is the dimensionless radial coordinate of the tip of the fin. $l^* = R_1 - \hat{R}$ in Fig. 4 is the dimensionless fin height [3].

b. Energy Equation:

The energy equation in dimensionless form is given below, with all conditions given in [6] also.

The energy equation governing the convective heat transfer in the flow of a viscous, incompressible, constant-property fluid with negligible viscous dissipation is recalled to be given as

$$\frac{1}{k}u\frac{\partial T}{\partial Z} = \frac{1}{r}\frac{\partial}{\partial r}\left(r\frac{\partial T}{\partial r}\right)+\frac{1}{r^2}\frac{\partial^2 T}{\partial \phi^2}+\frac{\partial^2 T}{\partial r^2}, \qquad (9)$$

where u is the velocity distribution appearing as an unknown solution of the momentum equation (8). This is solved in the domain shown in Fig. 4, subject to the following boundary conditions.

Constant heat flux boundary conditions imply

$$T = T_w(z) \text{ at } \phi = \alpha,\ r_i \le r \le r,$$

and

$$T = T_w(z) \text{ at } r = r_i,\ \alpha \le \phi \le \alpha+\beta,$$

where T_w is the temperature of the inner-pipe wall and also of the fin surface because of the assumption of infinite conductivity of the fin. This varies axially by virtue of the

1978 ISSN 1013-5316;CODEN: SINTE 8 Sci.Int.(Lahore),28(2),1975-1986 ,2016

boundary conditions. An adiabatic wall temperature condition at the outer pipe implies

$$\frac{\partial T}{\partial \phi} = 0 \text{ at } r = r_0\ ,\ 0 \le \phi \le \alpha + \beta.$$

Symmetry conditions at the lines of symmetry (so that there is no heat flux across these boundaries) ensure that

$$\frac{\partial T}{\partial \phi} = 0 \text{ at } \phi = 0,\ r_i \le r \le r_0, \qquad (10)$$

$$\frac{\partial T}{\partial \phi} = 0 \text{ at } \phi = \alpha + \beta,\ r_1 \le r \le r_0. \qquad (11)$$

The non-dimensional temperature distribution defined for the present situation, as

$$\tau^*(r,\phi) = \frac{T(r,\phi,z) - T_w(z)}{Q'/\lambda_I}. \qquad (12)$$

The above model can thus be converted into the dimensionless form

$$\frac{\partial^2 \tau^*}{\partial R^2} + \frac{1}{R}\frac{\partial^2 \tau^*}{\partial \phi^2} = \frac{u^*}{A_c^* \bar{u}^*}, \qquad (13)$$

where u^* is the velocity distribution obtained as a numerical solution of Eq. (6), A_c^* is the dimensionless free flow cross-sectional area and $\bar{u}^*$ is its mean value over A_c^* .

The boundary conditions given above can be written in terms of the dimensionless variables as

$$\tau^* = 0 \text{ at } R = \hat{R},\ 0 \le \phi \le \alpha,$$

$$\tau^* = 0 \text{ at } \phi = \alpha, \hat{R} \le R \le R_1,$$

$$\tau^* = 0 \text{ at } R = R_1,\ \alpha \le \phi \le \alpha + \beta,$$

$$\tau^* = 0 \text{ at } R = 1,\ 0 \le \phi \le \alpha + \beta,$$

$$\frac{\partial \tau^*}{\partial \phi} = 0 \text{ at } \phi = 0,\ \hat{R} \le R \le 1,$$

$$\frac{\partial \tau^*}{\partial \phi} = 0 \text{ at } \phi = \alpha + \beta,\ R_1 \le R \le 1.$$

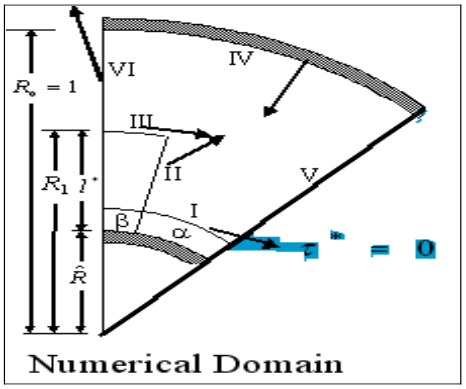

Fig.5

4. BODY-FITTED GRID GENERATION

Curvilinear grid generation, the solution domain and the boundary conditions are given and solution can be obtained by using grid of 41×21 as the situation described in the fig.6 to fig.8 and using body-fitted coordinate transformation technique, which was originally proposed by Thompson, et al. [8] & [21]and adopted by Cheng et al. and Syed et al. [4-6] respectively, is applied to generate curvilinear grid for computation at each iteration that

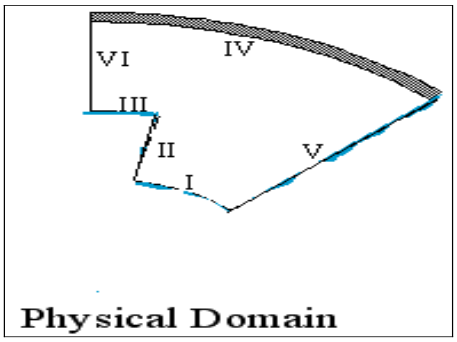

Fig.6

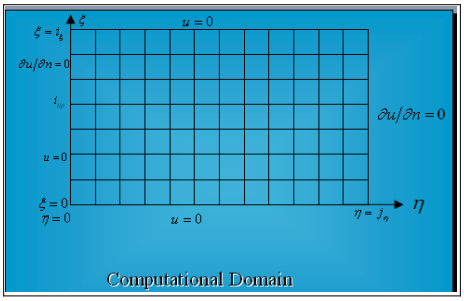

Fig.7

accommodates the variation of the shape of the solution domain during the optimization process. The grid generation method associated with the optimization process uses the framework of the numerical schemes proposed by Cheng and Wu [4] & [5]. The important features of the method are described below. The computational domain is defined by the coordinate transformation functions, $\xi = \xi(X,Y)$ and $\eta = \eta(X,Y)$, which are obtained by solving the following partial differential equations:

$$\frac{\partial^2 \xi}{\partial X^2} + \frac{\partial^2 \xi}{\partial Y^2} = F_1(\xi,\eta), \tag{14}$$

$$\frac{\partial^2 \eta}{\partial X^2} + \frac{\partial^2 \eta}{\partial Y^2} = F_2(\xi,\eta), \tag{15}$$

where $F_1(\xi,\eta)$ and $F_2(\xi,\eta)$ are two functions which are defined to artificially adjust the density of the grids locally, as suggested by Thompson, et al. [8] & [21]. Equations (14) and (15) are transformed into the computation domain as:

$$\begin{aligned} &\bar{\alpha}\frac{\partial^2 X}{\partial \xi^2} - 2\bar{\beta}\frac{\partial^2 X}{\partial \xi \partial \eta} + \bar{\gamma}\frac{\partial^2 X}{\partial \eta^2} \\ &= -J_a^2\left(F_1\frac{\partial X}{\partial \xi} + F_2\frac{\partial X}{\partial \eta}\right), \end{aligned} \tag{16}$$

$$\begin{aligned} &\bar{\alpha}\frac{\partial^2 Y}{\partial \xi^2} - 2\bar{\beta}\frac{\partial^2 Y}{\partial \xi \partial \eta} + \bar{\gamma}\frac{\partial^2 Y}{\partial \eta^2} \\ &= -J_a^2\left(F_1\frac{\partial Y}{\partial \xi} + F_2\frac{\partial Y}{\partial \eta}\right), \end{aligned} \tag{17}$$

where

$$\bar{\alpha} = \left(\frac{\partial X}{\partial \eta}\right)^2 + \left(\frac{\partial Y}{\partial \eta}\right)^2,$$

$$\bar{\beta} = \left(\frac{\partial X}{\partial \xi}\frac{\partial X}{\partial \eta}\right) + \left(\frac{\partial Y}{\partial \xi}\frac{\partial Y}{\partial \eta}\right),$$

$$\bar{\gamma} = \left(\frac{\partial X}{\partial \xi}\right)^2 + \left(\frac{\partial Y}{\partial \xi}\right)^2,$$

$$J_a = \left(\frac{\partial X}{\partial \xi}\frac{\partial Y}{\partial \eta}\right) - \left(\frac{\partial Y}{\partial \xi}\frac{\partial X}{\partial \eta}\right),$$

and J_a denotes the Jacobean of the transformation.

Once the solutions of $X(\xi,\eta)$ and $Y(\xi,\eta)$ are carried out in the computation domain from Equations (16) and (17), the transformation functions $\xi(X,Y)$ and $\eta(X,Y)$ can be obtained through an inverse mapping process.

The shape functions of the left boundary $X(\xi,\eta)$ and $Y(\xi,\eta)$, are iteratively up dated during the optimization process. Based on the updated functions, equations (16) and (17) are solved by the finite-difference method to yield the grid that accommodates the variation of the shape of the solution domain in iteration. Local orthogonality of the grid lines near boundaries can be ensured by simply setting

$$\beta = \left(\frac{\partial X}{\partial \xi}\frac{\partial X}{\partial \eta}\right) + \left(\frac{\partial Y}{\partial \xi}\frac{\partial Y}{\partial \eta}\right) = 0, \tag{18}$$

at these boundaries.

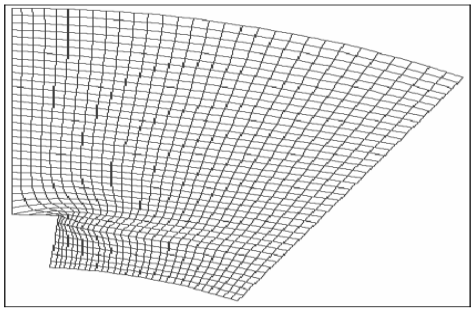

Grid 41 ×21

Fig.8

5. COMPUTATIONAL FORM OF THE MOMENTUM AND ENERGY EQUATIONS

Computational form of momentum and energy equations are as follows and also derived in [6].

a. Momentum Equation

$$\begin{aligned} &\alpha_1 u_{\xi\xi} + \alpha_1 u_{\eta\eta} - \alpha_1 u_{\xi\eta} + \alpha_4 u_{\xi} + \alpha_5 u_{\eta} \\ &= -\frac{4}{c}. \end{aligned} \tag{19}$$

The boundary conditions are as under :

(a) No slip conditions at the solid boundaries

$$u = 0 \text{ at } \xi = 0,\ 0 \le \eta \le j_\eta,$$

$$u = 0 \text{ at } \xi = i_\xi,\ 0 \le \eta \le j_\eta,$$

$$u = 0 \text{ at } \xi = i_{tip},\ 0 \le \eta \le j_\beta,$$

$$u = 0 \text{ at } \eta = j_\beta,\ 0 \le \xi \le i_{tip}.$$

(b) Symmetry conditions

$$\frac{\partial u}{\partial \eta} = \frac{R\eta}{R_\xi}\frac{\partial u}{\partial \xi} \text{ at } \eta = 0,\ i_{tip} \le \xi \le i_\xi,$$

and

$$\frac{\partial u}{\partial \eta} = \frac{R\eta}{R_\xi}\frac{\partial u}{\partial \xi} \text{ at } \eta = j_\eta,\ 0 \le \xi \le i_\xi,$$

1980 ISSN 1013-5316;CODEN: SINTE 8 Sci.Int.(Lahore),28(2),1975-1986 ,2016

where i_{tip} is the number of grid points in ξ direction till fin tip, i_ξ is the total number of grid points in ξ direction, $j_\in$ and j_ξ are the grid points on the fin tip and total number of grid points in ξ direction.

b. Energy equation

$$\alpha_1\tau_{\xi\xi}+\alpha_2\tau_{\xi\eta}+\alpha_4\tau_\xi+\alpha_5\tau_\eta=\frac{u}{Au}. \tag{20}$$

The transformed boundary conditions are

(a) At the solid boundaries

$$\begin{aligned}&\tau=0 \text{ at } \xi=0,\ 0\le\eta\le j_\eta,\\ &\tau=0 \text{ at } \xi=i_\xi,\ 0\le\eta\le j_\eta,\end{aligned} \tag{21}$$

$$\begin{aligned}&\tau=0 \text{ at } \xi=i_{tip},\ 0\le\eta\le j_\beta,\\ &\tau=0 \text{ at } \eta=j_\beta,\ 0\le\xi\le i_{tip},\end{aligned} \tag{22}$$

$$\frac{\partial\tau}{\partial\xi}=\frac{\theta_\xi}{\theta_\eta}\frac{\partial\tau}{\partial\eta} \text{ at } \xi=i_\xi,\ 0\le\eta\le j_\eta. \tag{23}$$

(b) Symmetry conditions

$$\frac{\partial\tau}{\partial\eta}=\frac{R\eta}{R_\xi}\frac{\partial\tau}{\partial\xi} \text{ at } \eta=0,\ i_{tip}\le\xi\le i_\xi, \tag{24}$$

and

$$\frac{\partial\tau}{\partial\eta}=\frac{R\eta}{R_\xi}\frac{\partial\tau}{\partial\xi} \text{ at } \eta=j_\eta,\ 0\le\xi\le i_\xi, \tag{25}$$

where for both above equations coefficients are as follows

$$\begin{aligned}&\alpha_1=\frac{r\theta_\eta^2+r_\eta^2}{g},\ \alpha_2=\frac{r\theta_\xi^2+r_\xi^2}{g},\\ &\alpha_3=\frac{2}{g}\left[r^2\theta_\xi\theta_\eta+r_\xi r_\eta\right],\end{aligned} \tag{26}$$

$$\begin{aligned}&\alpha_4=r_\eta\beta_5-\theta_\eta\beta_6,\ \alpha_5=\theta_\xi\beta_6-r_\xi\beta_5,\\ &\beta_1=\theta_{\xi\xi}\theta_\eta^2-2\theta_\xi\theta_\eta\theta_{\xi\eta}+\theta_{\eta\eta}\theta_\xi^2,\end{aligned} \tag{27}$$

$$\begin{aligned}&\beta_2=r_{\xi\xi}\theta_\eta^2-2r_{\xi\eta}\theta_\xi\theta_\eta+r_{\eta\eta}\theta_\xi^2,\\ &\beta_3=\theta_{\xi\xi}r_\eta^2-2\theta_{\xi\eta}r_\xi r_\eta+\theta_{\eta\eta}r_\xi^2,\end{aligned} \tag{28}$$

$$\begin{aligned}&\beta_4=r_{\xi\xi}r_\eta^2-2r_{\xi\eta}r_\xi r_\eta+r_{\eta\eta}r_\xi^2,\\ &\beta_5=\frac{r^3\beta_1+r\beta_3}{j\alpha^3},\\ &\beta_6=\frac{r^3\beta_2}{j\alpha^3}-\frac{1}{j\alpha}+\frac{r\beta_4}{j\alpha^3}.\end{aligned} \tag{29}$$

Problem; considering the cross sectional, laminar forced convection heat transfer in the finned double pipe Fig.2 as discussed earlier.

The target is to optimize shape design of the fin for a given Nusselt number. The momentum and energy equations in (ξ,η) computational domain are as (19) & (20) and boundary conditions are given above (21-29) .

6. SHAPE DESIGN PROCESS

The shape profiles of the medium domain represented by the shape functions $X(\xi,\eta)$ and $Y(\xi,\eta)$ are varied in order that the objective functional J , defined as:

$$J=\left(\int_1^N\tau_{n,j}-Nu\right)^2, \tag{30}$$

where

$$\tau_{n,j}=\frac{Dh}{(p_h)\times(T_b^*)}\times\frac{dT_{n,j}}{dN}, \tag{31}$$

is minimized, where Nu is the specified Nusselt number. Minimization of the objective function J is achieved by using the conjugate gradient method. Incorporated with a sensitivity analysis, the conjugate gradient method evaluates the gradients of the objective function and sets up a new conjugate direction for the updated solutions. In general, the convergence can be attained in a finite number of iterations. The construction of conjugate gradients for the test problem is discussed only briefly in the following:

Let $r_{n,j}^n$ and $\theta_{n,j}\ (j=1,2,3\ldots,n)$ be the nth iterative values of the shape functions $r(\eta)$ and $\theta(\eta)$ for grid point j on the left boundary and let the first search direction toward the minimization be the steepest descent direction in terms of the gradient functions:

$$\frac{\partial j}{\partial r_{n,j}}=2\left(\int_1^N\tau_{n,j}-Nu\right)\int_1^N\frac{\partial\tau_{n,i}}{\partial r_{n,j}}, \tag{32}$$

$$\frac{1}{r}\frac{\partial j}{\partial\theta_{n,j}}=2\left(\int_1^N\tau_{n,j}-Nu\right)\int_1^N\frac{1}{r}\frac{\partial\tau_{n,i}}{\partial\theta_{n,j}}, \tag{33}$$

where the terms $\frac{\partial\tau_{n,i}}{\partial r_{n,j}}$ and $\frac{\partial\tau_{n,i}}{\partial\theta_{n,j}}$ are referred to as the

Sci.Int.(Lahore),28(2),1967-1978 ,2016 ISSN 1013-5316;CODEN: SINTE 8

sensitivity coefficients. The task of the sensitivity analysis is to evaluate the sensitivity of objective function J with respect to the shape functions $r_b(\eta_i)$ and $\theta_b(\eta_i)$ to do this, the sensitivity coefficient must be known.

In this study, the terms $\frac{\partial \tau_{n,i}}{\partial r_{n,j}}$ and $\frac{\partial \tau_{n,i}}{\partial \theta_{n,j}}$ are calculated by introducing small perturbations to r and θ coordinates of each left boundary points individually. The grid generation for the perturbed shape is carried out, and the temperature solutions of the heat convection equations (19) and (20) are solved. By using the obtained temperature solutions, the dependence of the temperature at the point $j(\tau_{n,i})$ on the perturbation of the coordinates of point j can be evaluated and hence

$$\frac{\partial \tau_{n,i}}{\partial r_{n,j}} \text{ and } \frac{\partial \tau_{n,i}}{\partial \theta_{n,j}} \tag{34}$$

can be determined. This method is referred to as the "direct differentiation method". It is direct and accurate but is suitable only for problems with a small number of shape variables. For those with a large number of shape variables, the sensitivity analysis may become a somewhat time consuming step. In that case a reanalysis method proposed by Kirsch [17] may be used as an aid to reduce the computation time. In addition, the ad-joint variable method described by Meric [18] and Dems and Mroz [19] can also be applied. This type of method provides an analytical sensitivity expression for shape design and is especially suited to problems with a small number of systems behaviors functional but a large number of shape parameters. Meanwhile, the discretization of the system equations for optimization is not necessary with this method. However, the shape design sensitivity expression is dependent on the problem and its mathematical model, and one needs to derive different analytical expressions when considering different systems. For those cases for which the system behavior contrast to the ad-joint variable method, the direct method requires much less mathematical implementation, and therefore the application of the direct method is not limited to any specific system or mathematical formulation. Based on the conjugate gradient scheme, the coordinate of the point j on the left boundary be updated by

$$r_{n,j}^{n+1} = r_{n,j}^{n} - \beta_j p_{j,r}^{n} \tag{35}$$

$$\theta_{n,j}^{n+1} = \theta_{n,j}^{n} - \beta_j p_{j,\theta}^{n} \tag{36}$$

for $j = 1, 2, 3....n,$ where the search direction $p_{j,r}^{n}$ and $p_{j,\theta}^{n}$ are expressed as a linear combination of the steepest descent directions and a vector, that is:

$$p_{j,r}^{n} = \frac{\partial j}{\partial r_{n,j}} + \gamma_{j,r}^{n}\ p_{j,r}^{n-1}, \tag{37}$$

$$p_{j,\theta}^{n} = \frac{1}{r}\frac{\partial j}{\partial \theta_{n,j}} + \gamma_{j,\theta}^{n}\ p_{j,\theta}^{n-1}, \tag{38}$$

for $j = 1, 2, \ldots, n$ where (steepest --descent directions) are given as:

$$p_{j,r}^{0} = -\frac{\partial j}{\partial r_{n,j}}, \tag{39}$$

$$p_{j,\theta}^{0} = -\frac{\partial j}{r\partial \theta_{n,j}}, \tag{40}$$

for $j = 1, 2, \ldots, n.$

6.1. CONJUGATE GRADIENT COEFFICIENTS

The conjugate gradient coefficients $\gamma_{j,r}^{n}$ and $\gamma_{j,\theta}^{n}$ are calculated by

$$\gamma_{j,r}^{n} = \left[\left(\frac{\partial j}{\partial r_{n,j}} \right)^{n} / \left(\frac{\partial j}{\partial r_{n,j}} \right)^{n-1} \right]^2, \tag{41}$$

$$\gamma_{j,\theta}^{n} = \left[\left(\frac{\partial j}{r\partial \theta_{n,j}} \right)^{n} / \left(\frac{\partial j}{r\partial \theta_{n,j}} \right)^{n-1} \right]^2, \tag{42}$$

for $j = 1, 2, \ldots, n.$

6.2. CALCULATIONS OF STEP SIZE

The step size $\beta_j\ (j = 1, 2, \ldots, n)$ appearing in equations (35) and (36) are to be determined. The value of β_j are selected to minimize the updated objective function J^{n+1}. With the help of equations (32, 33, 35) and (36) and the Taylor's series expression, the $(n+1)th$ objective function is given by

$$J^{n+1} = \left[\int_1^N \tau_{n,i}^{n+1} \left(\begin{matrix} r_{1,j}^{n} - \beta_1 p_{1,r}^{n}, r_{2,j}^{n} - \beta_2 p_{2,r}^{n}, ..., r_{n,j}^{n} \\ - \beta_n p_{n,r}^{n}, \theta_{1,j}^{n} - \beta_1 p_{1,\theta}^{n}, \theta_{2,j}^{n} \\ - \beta_2 p_{2,\theta}^{n}, ..., \theta_{n,j}^{n} - \beta_n p_{n,\theta}^{n} \end{matrix} \right) - Nu \right]^2$$

$$= \left[\left(\int_1^N \tau_{n,i}^n - Nu \right) - \int_1^N \left(\begin{array}{l} \beta_1 p_{1,r}^n \dfrac{\partial \tau_{n,i}}{\partial r_{1,j}} + \beta_2 p_{2,r}^n \dfrac{\partial \tau_{n,i}}{\partial r_{2,j}} + \\ \ldots + \beta_n p_{n,r}^n \dfrac{\partial \tau_{n,i}}{\partial r_{n,j}} \end{array} \right) ds \right. \quad (43)$$

$$\left. - \int_1^N \frac{1}{r} \left(\begin{array}{l} \beta_1 p_{1,\theta}^n \dfrac{\partial \tau_{n,i}}{\partial \theta_{1,j}} + \beta_2 p_{2,\theta}^n \dfrac{\partial \tau_{n,i}}{\partial \theta_{2,j}} + \\ \ldots + \beta_n p_{n,\theta}^n \dfrac{\partial \tau_{n,i}}{\partial \theta_{n,j}} \end{array} \right) ds \right]^2,$$

setting the derivatives of J^{n+1} with respect to β_j equal to zero

$$\frac{\partial J^{n+1}}{\partial \beta_j} = 0, \quad (44)$$

i.e.

$$\int_1^N \left[\sum_{k=1}^n \beta_k \int_1^N \left(p_{k,r}^n \frac{\partial \tau_{n,i}}{\partial r_{n,k}} + p_{k,\theta}^n \frac{\partial \tau_{n,i}}{r \partial \theta_{n,j}} \right) ds \right] \times \int_1^N \left(p_{j,r}^n \frac{\partial \tau_{n,i}}{\partial r_{n,j}} + p_{j,\theta}^n \frac{\partial \tau_{n,i}}{r \partial \theta_{n,j}} \right) ds \quad (45)$$

$$= \left(\sum_{i=1}^n \tau_{n,i}^n - Nu \right) \int_1^N \left(p_{j,r}^n \frac{\partial \tau_{n,i}}{\partial r_{n,j}} + p_{j,\theta}^n \frac{\partial \tau_{n,i}}{r \partial \theta_{n,j}} \right) ds,$$

for $j = 1, 2, \ldots n.$

Equation (43) represents a set of linear algebraic equations which could be solved simultaneously to obtain the optimal step size β_j $(j = 1, 2, \ldots, n)$. The solution can be performed numerically by means of Gaussian Elimination method. The equation becomes as

$$\sum_{k=1}^n \left[\sum_{k=1}^n \beta_k \int_1^N \left(p_{k,r}^n \frac{\partial \tau_{n,i}}{\partial r_{n,k}} + p_{k,\theta}^n \frac{\partial \tau_{n,i}}{r \partial \theta_{n,j}} \right) ds \right] \times \int_1^N \left(p_{j,r}^n \frac{\partial \tau_{n,i}}{\partial r_{n,j}} + p_{j,\theta}^n \frac{\partial \tau_{n,i}}{r \partial \theta_{n,j}} \right) ds \quad (46)$$

$$= \left(\int_1^N \tau_{n,i}^n - Nu \right) \int_1^N \left(p_{j,r}^n \frac{\partial \tau_{n,i}}{\partial r_{n,j}} + p_{j,\theta}^n \frac{\partial \tau_{n,i}}{r \partial \theta_{n,j}} \right) ds,$$

for $j = 1, 2, \ldots n.$

These are n equations with n unknown β's. These equations become in matrices form

$$A_{n \times n} \beta_{n \times 1} = B_{n \times 1}, \quad (47)$$

where each element of $A_{n \times n}$ is as

$$a(l,m) = \sum_{i=1}^n \int_1^N \left(p_{m,r}^n \frac{\partial \tau_{n,i}}{\partial r_{n,m}} + p_{m,\theta}^n \frac{\partial \tau_{n,i}}{r \partial \theta_{n,m}} \right) ds \times \int_1^N \left(p_{l,r}^n \frac{\partial \tau_{n,i}}{\partial r_{n,l}} + p_{l,\theta}^n \frac{\partial \tau_{n,i}}{r \partial \theta_{n,l}} \right) ds, \quad (48)$$

for $r = 1, 2, \ldots, n$ and $m = 1, 2, \ldots, n$ each element of $B_{N \times 1}$ is as

$$b_{l \times 1} = \left(\int_1^N \tau_{n \times i}^n - Nu \right) \times \int_1^N \left(p_{l,r}^n \frac{\partial \tau_{n,i}}{\partial r_{n,l}} + p_{l,\theta}^n \frac{\partial \tau_{n,i}}{r \partial \theta_{n,l}} \right) ds \quad (49)$$

in both the above equations (48) and (49) and $l = 1, 2, \ldots, n$ & $m = 1, 2, \ldots, n.$

Equation (46) may be solved by any method and β_j may be calculated.

7. NEW OPTIMAL BOUNDARY

Putting the values of β_j in the following equations, we get new optimal shape

$$r_{n,j}^{n+1} = r_{n,j}^n - \beta_j p_{j,r}^n \quad (50)$$

$$\theta_{n,j}^{n+1} = \theta_{n,j}^n - \beta_j p_{j,\theta}^n \quad (51)$$

for $j = 1, 2, \ldots, n.$

a. STEPS FOR THE PROCESS

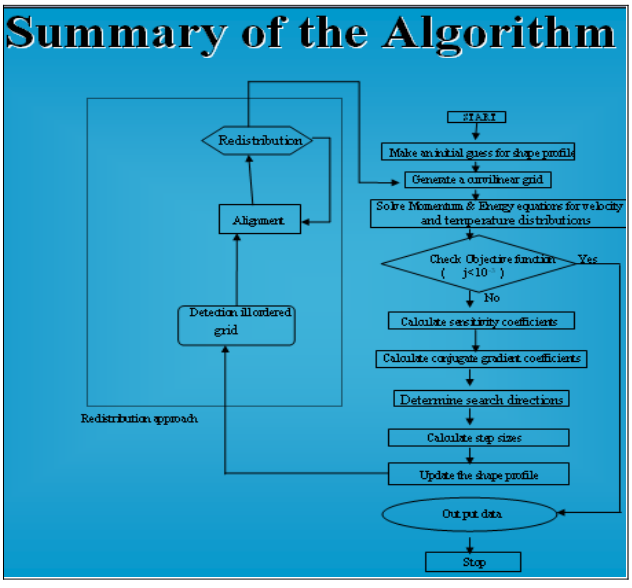

Fig.9

Sci.Int.(Lahore),28(2),1967-1978 ,2016 ISSN 1013-5316;CODEN: SINTE 8

RESULTS

Tables for 6 fins 10 % , 20% , 30% , 40% , & 50% Increase in Nusselt number

Table # 2 No. of fins = 6, 20% Increase of Nu

H	Initial Shape		First		second		third		fourth	
	Nub	Nu	Nub	Nu	Nub	Nu	Nub	Nu	Nub	Nu
0.2	4.70529	20.70319	--	--	--	--	--	--	--	--
0.3	4.43486	22.39262	5.29533	24.13713	congratulations					
0.4	4.33436	24.69909	--	--	--	--	--	--	--	--
0.5	4.29898	27.21381	--	--	--	--	--	--	-	-
0.6	4.11780	28.71510								

H	initial		first		second		third		fourth	
	λ	Q	λ	Q	λ	Q	λ	Q	λ	Q
0.2	.5	1.00983	--	--	--	---	---	---	--	--
0.3	.45	1.00794	.52	1.09513	congratulations					
0.4	.45	1.00958	--	--	--	--	--	--	--	--
0.5	00	1.01301								
0.6	00	1.02378								

Table # 3 No. of fins = 6, 30% Increase of Nu

H	Initial Shape		First		second		third		fourth	
	Nub	Nu	Nub	Nu	Nub	Nu	Nub	Nu	Nub	Nu
0.2	4.70529	20.70319	4.98269	19.75198	--	--	--	--	--	--
0.3	4.43486	22.39262	4.90971	22.32257	4.92527	22.38343	4.84525	22.03385	--	--
0.4	4.33436	24.69909	4.59377	23.68359	4.55124	23.40857	4.62437	23.70533	4.67466	24.03403
0.4	4.63491	23.78502	5.65850	29.07074	--	--	--	--	--	--
.5	4.29898	27.21381	--	--	--	--	--	--	-	-
.6	4.11380	28.71510	--	--	--	--	--	--	--	--

H	initial		first		second		third		fourth	
	λ	Q	λ	Q	λ	Q	λ	Q	λ	Q
0.2	.5	1.00983	.25	1.00492	--	--	--	--	--	--
0.3	.45	1.00794	.99	1.00327	.94	1.00382	.9	1.00040	--	--
0.4	.45	1.00958	.85	1.00389	.6	1.00147	.88	1.00522	.93	1.00893
0.4	.88	1.00260	.78	1.20750	--	--	--	--	--	--
0.5	00	1.01302	--	--	--	--	--	--	-	-
0.6	00	1.02378	--	--	--	--	--	--	--	--

Table # 4 No. of fins = 6, 40% Increase of Nu

H	Initial Shape		First		second		third		fourth	
	Nub	Nu	Nub	Nu	Nub	Nu	Nub	Nu	Nub	Nu
0.2	4.68469	20.61258	--	--	--	--	--	--	--	--
0.3	4.43486	22.39262	--	--	--	--	--	--	--	--
0.4	4.33057	24.67752	4.57649	23.67542	4.60777	23.74837	4.68784	24.06467	4.61301	23.67124
0.5	4.29898	27.21381	--	--	--	--	--	--	--	--
0.6	4.11380	28.71510	--	--	--	--	--	--	--	--

H	initial		first		second		third		fourth	
	λ	Q	λ	Q	λ	Q	λ	Q	λ	Q
0.2	.45	1.0055	error	--	--	--	--	--	--	--
0.3	.45	1.00794	--	---	--	--	--	--	--	--
0.4	.78	1.00817	.81	1.00418	.88	1.00187	.81	1.00287	.81	1.00248
0.5	00	1.01302	--	--	--	--	--	--	--	--
0.6	00	1.02378	--	--	--	--	--	--	--	--

Table # 5 No. of fins = 6, 50% Increase of Nu

H	Initial Shape		First		second		third	
	Nub	Nu	Nub	Nu	Nub	Nu	Nub	Nu
0.2	4.68469	20.61258	5.28917	20.97519	5.40301	21.41975	5.49459	21.81711
0.3	4.43486	22.39262	--	--	--	--	--	--
0.4	4.32817	24.66383	4.60509	23.9019	--	--	--	--
0.5	4.29898	27.21381	--	--	--	--	--	--
0.6	4.11380	28.71510	--	--	--	--	--	--

H	initial		first		second		third	
	λ	Q	λ	Q	λ	Q	λ	Q
0.2	.45	1.00550	1.00	.98797	.99	1.0088	1.00	1.02749
0.3	.45	1.00794	--	--	--	--	--	--
0.4	.82	1.00710	.89	1.00736	--	--	--	--
0.5	00	1.01302	--	--	--	--	--	--
0.6	00	1.02378	--	--	--	--	--	--

No of Fins_6, Fin Height_40% of Annulus, Fin Half Angle_5deg,

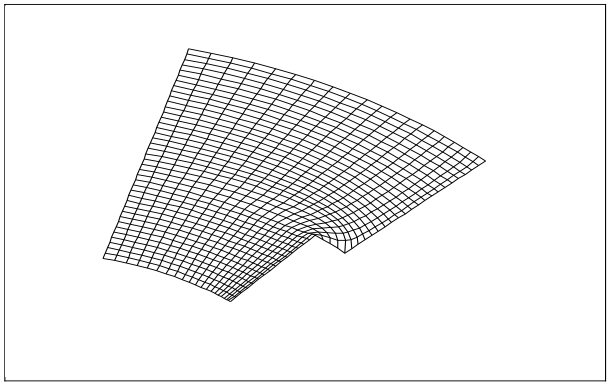

$$\overline{Nu} = 4.33436$$

Initial Shape with Body Fitted Grid

Fig. 10

No of Fins_6, Fin Height_40% of Annulus, Fin Half Angle_5deg

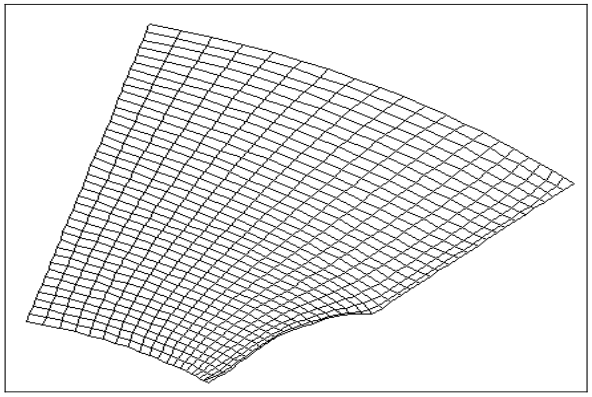

$$\overline{Nu} = 4.59679$$

6% increase relative to initial shape

First Shape with body fitted grid

Fig . 11

No of Fins_6, Fin Height_40% of Annulus, Fin Half Angle_5deg

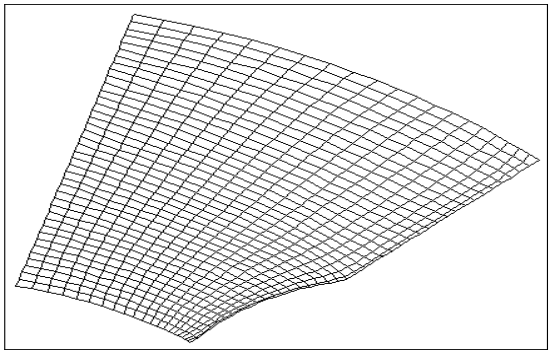

$\overline{Nu} = 4.79867$

4.4% increase relative to first shape

10.7% increase relative to initial shape

Second Shape with body fitted grid

Fig .12

Tables for 12 fins 10 %, 20%, 30%, 40%, & 50% Increase in Nusselt number

Table # 6 No. of fins = 12, 10% Increase of Nu

H	Initial Shape		First		second		third	
	Nub	Nu	Nub	Nu	Nub	Nu	Nub	Nu
0.2	3.54071	20.03470	--	--	--	--	--	--
0.3	3.08451	21.4585	--	--	--	--		
0.4	2.99145	24.69533	3.42823	24.73547	--	--	--	--
0.5	3.32851	31.68410	--	--	--	--	--	--

H	Initial		first		second		third	
	λ	Q	λ	Q	λ	Q	λ	Q
0.2	.87	.99433	--	--	--	--	--	--
0.3	.67	.97647	--	---	--	--		
0.4	.75	.97506	.77	1.00303	--	--	--	--
0.5	.3	1.00245	--	--	--	--	--	--

Table # 7 No. of fins = 12, 20% Increase of Nu

H	Initial Shape		First		second		third		
	Nub	Nu	Nub	Nu	Nub	Nu	Nub	Nu	
0.2	3.54071	20.0370	4.26815	20.45954	Congratulations				
0.3	3.08309	21.44856	--	--	--				
0.4	2.99128	24.69791	3.40756	24.69513	3.59884	25.60257	Congratulations		
0.5	3.32851	31.68410	--	--	--	--	-	--	- -

H	Initial		first		second		third	
	λ	Q	λ	Q	λ	Q	λ	Q
0.2	.87	.99433	.81	1.00534	--	--	--	--
0.3	.97	.96720	--	--				
0.4	.77	.97468	.8	1.00178	.87	1.02101	--	--
0.5	.3	1.00245	--	--	--	--	--	--

Table # 8 No. of fins = 12, 30% Increase of Nu

H	Initial Shape		First		second		third		fourth	
	Nub	Nu	Nub	Nu	Nub	Nu	Nub	Nu	Nub	Nu
0.2	3.54071	20.0347	--	--	--	--	--	--	--	--
0.3	3.09381	21.52322	3.81366	22.66361	--	--	--	--	--	--
0.4	2.99108	24.69220	3.49254	25.05631	3.51036	25.02664	3.57835	25.44457	3.59481	25.53300
0.5	3.32851	31.68410	--	--	--	--	--	--	--	--

H	Initial		first		second		third		fourth	
	λ	Q	λ	Q	λ	Q	λ	Q	λ	Q
0.2	.87	.99433	--	--	--	--	--	--	--	--
0.3	.87	.97519	.72	1.00812	--	--	--	--	--	--
0.4	.69	.97545	.85	1.00656	.7	1.00736	.83	1.001.5	.84	1.00596
0.4										
0.5	.3	1.00245	--	--	--	--	--	--	--	--

Table # 9 No. of fins = 12 40% Increase of Nu

H	Initial Shape		First		second		third		fourth	
	Nub	Nu	Nub	Nu	Nub	Nu	Nub	Nu	Nub	Nu
0.2	3.54071	20.03470	4.13457	19.82580	--	--	--	--	--	--
0.3	3.06934	21.35297	--	--	--	--	--	--	--	--
0.4	2.99090	24.69078	3.42134	24.74415	3.48110	24.88617	3.51157	25.11167	3.60088	25.5624
0.5	3.32851	31.68410	--	--	--	--	--	--	--	--
0.6										

H	Initial		first		second		third		fourth	
	λ	Q	λ	Q	λ	Q	λ	Q	λ	Q
0.2	.87	.9433	.62	1.00745	--	--	--	--	--	--
0.3	.57	.97151	--	--	--	--	--	--	--	--
0.4	.69	.97545	.84	1.00380	.8	1.00769	.86	1.00809	.84	1.00176
0.5	.3	1.00245	--	--	--	--	--	--	--	--

Table # 10 No. of fins = 12, 50% Increase of Nu

H	Initial Shape		First		second		third		fourth	
	Nub	Nu	Nub	Nu	Nub	Nu	Nub	Nu	Nub	Nu
0.2	3.54071	20.03470	4.21333	20.18733	--	--	--	--	--	--
0.3	3.09220	21.51202	--	--	--	--	--	--	--	--
0.4	2.99128	24.69291	3.43186	24.69756	3.5270	25.21018	3.56920	25.50052	3.57314	25.44800
0.4	3.58284	25.38915	--	--	--	--	--	--	--	--
0.5	3.32851	31.68410	--	--	--	--	--	--	--	--

H	Initial		first		second		third		fourth	
	λ	Q	λ	Q	λ	Q	λ	Q	λ	Q
0.2	.87	.99433	.73	1.00693	--	--	--	--	--	--
0.3	.91	.97436	--	--	--	--	--	--	--	--
0.4	.77	.97468	.83	1.00412	.86	1.00432	.89	1.00631	.92	1.00832
0.4	.85	1.00158	--	--	--	--	--	--	--	--
0.5	.3	1.00245	--	--	----	--	---	--	--	--

No of Fins_12, Fin Height_40% of Annulus, Fin Half Angle_5deg

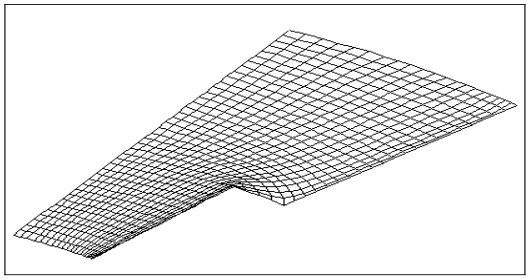

$\overline{Nu} = 2.99128$

Initial Shape with Body Fitted Grid

Fig. 13

No of Fins_12, Fin Height_40% of Annulus, Fin Half Angle_5deg

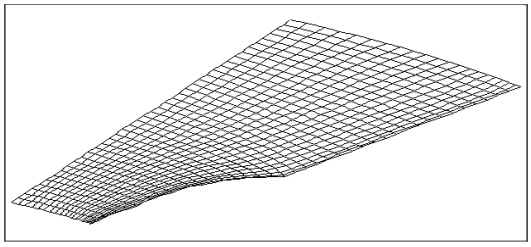

$\overline{Nu} = 3.40756$

13.9% increase relative to initial shape

First Shape with body fitted grid

Fig. 14

Sci.Int.(Lahore),28(2),1967-1978 ,2016 ISSN 1013-5316;CODEN: SINTE 8

No of Fins_12, Fin Height_40% of Annulus,
Fin Half Angle_5deg

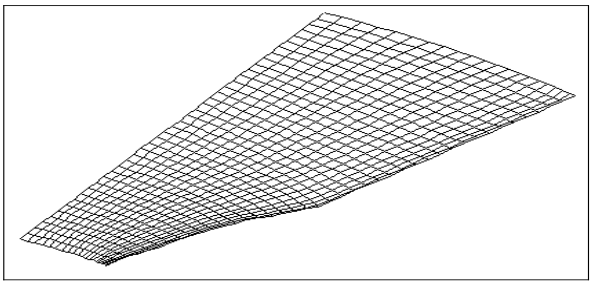

$\overline{Nu} = 3.59884$

5.6% increase relative to first shape
20% increase relative to initial shape
Second Shape with body fitted grid

Fig. 15

8. DISCUSSION

A computational procedure based on body fitted generation, steady conjugate gradient method and grid redistribution scheme has been employed to examine the shape design of a finned double pipe for optimal thermal performance. The iterative scheme is presented in fig. 9 .

The results for six fins with 10% , 20% , 30% , 40% and 50% increase in Nusselt number have been tabulated in the tables 1 to 5 .

It has been noted that the results for 10% and 20% increase have been successfully achieved as shown in the table. 1 and table. 2 . The results for 30% , 40% and 50% increase in thermal performance could not be achieved as depicted in table. 3 to table. 5 .

We can see from the table. 1 that 10% increase of the Nu is achieved after second iteration, when the fin height H is 30% of the original height, the basic Nusselt number Nu is 4.43486 and specified Nusselt number w.r.t. initial shape is 22.39262 , the heat conduction parameter l is increased from 0.45 to 0.94 and Q the quantity of heat transferred drops from 1.00794 to 0.99740 . Similarly, table. 2 shows that 20% increase of the Nu is achieved after first iteration, when the fin height H is 30% of the original height, the basic Nusselt number Nu is 4.43486 and specified Nusselt number w.r.t. initial shape is 22.39262 , the heat conduction parameter l is increased from 0.45 to 0.52 and Q the quantity of heat transferred increases from 1.00794 to 1.09513 .

Fig. 10 presents the initial shape with body fitted grids, when the number of fins is 6 , fin height is 40% of the annulus and the fin angle is 5 degrees. Fig. 11 and fig. 12 respectively depict the shape of fin with an increase of 6% and 10.7% to the thermal performance as compared to the shape of initial fin as shown in fig.10.

Table 6 to table 10 contains the results when the number of fins is 12 . Table 7 shows that Nusselt number increases by 20% when the fin height is 20% as well as 40% of the original height. Fig. 13 shows the initial shape with body fitted grids when the number of fins is 12 . Fig. 14 and fig. 15 respectively depict the shape of fin with an increase of 13.9% and 20% to the thermal performance as compared to the shape of initial fin as shown in fig. 13 .

9. CONCLUSION

- It shows that model woks properly.
- Clearly Fig. 10 to Fig. 15 and table. 1 to table. 10 show the efficiency and successful computer implementation of the optimal design process.
- The above results are due to successful body-fitted grid generation.
- Conjugate gradient method performed excellently in the current problem.

ACKNOWLEDGMENT:

This project was supported by the deanship of scientific research at Majmaah University under the research project No. 26. The author is highly grateful to Majmaah University, Deanship of Scientific Research and Research Center for Engineering and Applied Sciences, Majmaah University for support and encouragement.

The author is also, obliged to College of Science in Al-Zulfi City, Majmaah University, KSA) for sparing to accomplish this work. The author would like to thank Deanship of Scientific Research, Majmaah University, Kingdom of Saudi Arabia for funding this work under project number No.1436-2-9. (26. 1436).

REFERENCES

[1] S. Gupta, Calculus of Variations with Applications, Prentice. Hall of India New Dehli,1997.

[2] M. Z. Hussain, Dissertation, M. Phil, Optimal Shape Design B. Z. U. MULTAN, 1992.

[3] K. S. Syed, Ph. D, thesis, Simulation of fluid flow through a double-pipe Heat Exchanger, department of mathematics, University of Brad Ford, U.K., 1997.

[4] Chin-Hsiang Cheng and Chun-Yin Wu, An Approach Combining Body Fitted Grid Generation and Conjugate Gradient Methods for Shape Design in Heat Conduction Problems ,Int. J. Numerical Heat Transfer, Part B, 37: 69-83, 2000.

[5] Chin-Hsien Lan, Chin-Hsiang Cheng and Chun-Yin Wu ,Shape Design for Heat Conduction Problems using Curvilinear grid Generation, Conjugate Gradient and Redistribution Methods, Int.J .Numerical Heat Transfer, Part A, 39: 487-510, 2001.

[6] K. S. Syed, Iqbal Mazhar and N. A. Mir, Convective heat transfer in the thermal entrance region of finned double-pipe, Heat Mass Transfer, 43, 449-457, 2007.

[7] G. Fabbri, Heat Transfer Optimization in Internally Finned Tubes under Laminar Flow Condition ,Int . J .heat Mass Transfer, 41, 1243-1253, 1998.

[8] J. F. Thompson, F. C. Thames ,and C. W. Mastin ,Boundary-fitted Curvilinear Coordinate System for Solution of Partial Differential Equation on Fields Containing Any Number of Arbitrary Two Dimensional Bodies, NASA CR-2729, 1976.

[9] C. H .Cheng and J. H. YU, Conjugate Heat Transfer and Buoyancy-Driven Secondary Flow in the Cooling Channels within a Vertical Slab ,Numerical Heat Transfer, part A, 28, 443-459, 1995.

[10] Y. P. Chang and M. H. Hu, Optimization of Finned Tubes for Heat Transfer in Laminar Flow, Int. J. Heat Transfer, 1973.

[11] G. D. Smith, Numerical Solution of Partial Differential Equations: finite Difference Methods, Oxford University Press, 1985.

[12] G. F. Carey, Computational Grids Generation : Adaptation and Solution Strategies ,Taylor & Francis 1101 Vermont Avenue, N .W. suit 200 Washington, DC 2005-3521, U.S.A, 1997.

[13] R. Fletcher,Practical Methods of Optimization John Wiley & sons Ltd ,Thompson Press Ltd ,New Delhi,India., 1987.

[14] U. Kirsch, Efficient reanalysis for Topological Optimization, structural optimisation, 6, 143-150, 1993.

[15] H. Rodrigues and P. Fernandes, A Material Based Model for Topology Optimization of Thermo elastic Structures, int. J. Numer. Meth. Eng, 6, 143-150, 1993.

[16] K. Loar and H. Kalman, Performance and Optimum Dimensions of Different Cooling Fins with a Temperature Dependent Heat Transfer Coefficient, int. J. Heat Mass Transfer, 40, 1993 -- 2003, 1996.

[17] G. Fabbri, A Genetic Algorithm for Fin Profile Optimization, int. J. Heat Mass Transfer, 40, 2165-2172, 1997.

[18] U. Krisch, Efficient Reanalysis for Topological Optimization, Structural Optomozation, 6, 143--150, 1993.

[19] R. A. Meric, Shape Design Sensitivity Analysis and Optimization for Non-linear Heat and Electric Conduction Problems, Numer .Heat Transfer A, 34, 185 -- 203, 1998.

[20] K. Dems and Z. Mroz, sensitivity Analysis and Optimal Design of External Boundaries and Interface for heat conduction Systems, J. Thermal Stresses, 21, 461--488, 1998.

[21] O. M. Alifanov, Inverse Heat Transfer Problems, Springer-Verlag, New York, 1994.

[22] J. F. Thompson, F. C. Thames and C . W. Mastin , Automatic Numerical Generation of Body-Fitted Curvilinear Coordinates System for Fields Containing Any Number of Arbitrary Two Dimensional Bodies, J . Coput. Phy., 15, 229--319, 1974.

[23] C. H. Cheng and C. C . Chao, Numerical Prediction of the buoyancy-Driven Flow in the Annulus between Horizontal Eccentric Elliptical Cylinders, Numer. Heat Transfer A, 30, 283--303, 1996.

[24] M. Hanke, Conjugate Gradient Type Methods for Ill-Passed Problems, Wiley, New York, 1995.

[25] C. Parakash, Y. D. Liu, Analysis of laminar flow and heat transfer in the entrance region of an internally finned circular duct. J Heat Transfer 107: 84--91, 1985.

[26] I. M. Rustum, H. M. Soliman, Numerical analysis of laminar forced convection in the entrance region of tubes with longitudinal internal fins. J Heat Transfer 110: 310--313, 1988.

[27] V. D. Sakalis, P. M. Hatzikonstantinou, Laminar heat transfer in the entrance region of internally finned square ducts. J Heat Transfer 123 (6):1030--1034, 2001.

[28] R. K. Shah, A. L. London, Laminar flow forced convection in ducts. Academic, London, 1978.